# The jamming transition as probed by quasistatic shear flow

Claus Heussinger and Jean-Louis Barrat
*Université de Lyon; Univ. Lyon I, Laboratoire de Physique de la Matière Condensée et Nanostructures; CNRS, UMR 5586, 69622 Villeurbanne, France*
(Dated: May 9, 2009)

We study the rheology of amorphous packings of soft, frictionless particles close to jamming. Implementing a quasistatic simulation method we generate a well defined ensemble of states that directly samples the system at its yield-stress. A continuous jamming transition from a freely-flowing state to a yield stress situation takes place at a well defined packing fraction, where the scaling laws characteristic of isostatic solids are observed. We propose that long-range correlations observed below the transition are dominated by this isostatic point, while those that are observed above the transition are characteristic of dense, disordered elastic media.

PACS numbers: 83.80.Fg,83.50.Ax,62.20.de

A collection of spherical particles, interacting via a finite-range repulsive (contact) potential, unjams from a solid to a non-rigid state when being decompressed below a critical volume-fraction, $\phi_c$ [1, 2]. This transition, which has been given the name "point J", is accompanied by several interesting and nontrivial scaling relations in the solid phase [1, 3]. There, pressure and linear elastic shear modulus vanish as does the ratio of shear to bulk modulus. The average number of particle contacts jumps from a finite value $z_0$ at point J to zero just below the transition. The value of $z_0$ is compatible with Maxwell's estimate for the rigidity transition and signals the fact that at point J each particle has just enough contacts for a rigid/solid state to exist (which is called "isostatic" state) [4, 5]. Above the transition, additional contacts are generated according to the surprisingly universal law, $\delta z \sim \delta\phi^{1/2}$. While the system moves away from its isostatic state the effective size of the remaining isostatic regions, $l^\star \sim \delta z^{-1}$ [6, 7] has been argued to provide the diverging length-scale that endows point J with a certain "criticality". Based on these findings, jamming has been regarded as a "mixed" transition that shares properties of both, discontinuous (jump in contact number) and continuous phase- transitions (diverging length-scale) [8, 9].

A different route to approach point J from the fluid phase has been used in the flow simulations of Refs. [10, 11, 12]. Several scaling relations have been reported, some of which depend on model details. Some others seem to share the universality encountered in the solid phase. In contrast to the linear elastic properties in the solid phase, only little understanding about the flow properties and their relation to nearby point J has been achieved up to now.

In this Letter, we employ a quasistatic simulation technique that studies the borderline between fluid and solid state. As we will see, it combines both aspects, the elasticity of a solid and the flow of a fluid, in one simulation. This fact allows us to get insight into how point J, and its isostatic state, affects the flow properties close by. In particular we show that jamming (i.e. the development of a finite shear stress) as probed by shear flow should be viewed as a continuous transition, with isostatic effects showing up in the flow properties primarily below the transition ($\phi < \phi_c$). In contrast, at volume-fractions above $\phi_c$ the flow is characteristic for amorphous, but well connected, materials.

The quasistatic simulation probes the flow of the system in the limit of vanishing shear rate, $\dot\gamma \to 0$ (see Fig. 1). On lowering the volume-fractions from values above $\phi_c$, point J is therefore approached along the yield-stress line. The resulting "yield-stress-flow" is generated by a succession of equilibrated solid states that, as we will see, carry the signature of the nearby isostatic state. At point J the yield stress vanishes such that at lower volume-fractions, $\phi < \phi_c$, the simulation follows the $\phi$-axis and the system flows at zero stress. This corresponds to the limiting case, $\dot\gamma \to 0$, of normal fluid flow in the Newtonian regime [10].

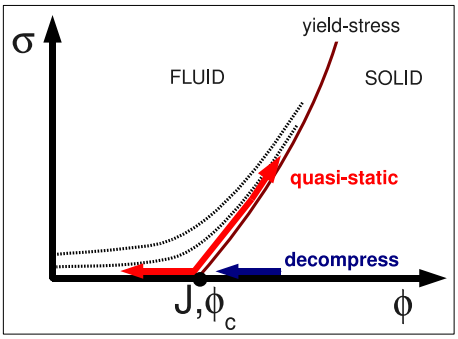


FIG. 1: Trajectory taken by quasistatic simulations in state-space of shear stress $\sigma$ and volume-fraction $\phi$. (Dotted lines) contours of constant strain rate $\dot\gamma$. The simulation corresponds to $\dot\gamma \to 0$ and thus follows the yield-stress line, $\sigma_y(\phi)$. Previous approaches either probe linear elasticity of the solid (decompression at $\sigma = 0$) or the steady-state flow of the fluid.

Our system consists of $N$ soft spherical particles that interact with an harmonic contact interaction with spring constant $k$. As in Refs. [1, 10, 13] we use a 50 : 50 mixture

of particles with radius $a$ and $1.4a$ in two dimensions. In the simulations the volume fraction $\phi$ is controlled, while stresses are allowed to fluctuate. Primary output are the pressure, $p$, and (shear-)stress $\sigma$ as a function of imposed strain, $\gamma$ (see Fig. 2). To implement the shear, variable Lee-Edwards boundary conditions are used. The simulation proceeds by minimizing the total potential energy (using conjugate gradient techniques [14]) after each affine change in the boundary conditions and particle coordinates, ($\Delta\gamma = 5{\cdot}10^{-5}$). Thus, as the energy landscape evolves under shear the system always remains at a local energy minimum, with all forces fully equilibrated.

As can be seen from Fig. 2 a typical feature of quasistatic stress-strain relations is the presence of elastic branches, where the stress grows linearly with strain. This reversible elastic loading is terminated by irreversible plastic events during which the stress drops rapidly and energy is dissipated. The succession of elastic and plastic events defines the flow of the material just above its yield-stress $\sigma_y(\phi)$. On lowering the volume-fraction the average stress-level decreases until, below $\phi_c$, it vanishes and the system flows at zero stress. For intermediate volume-fractions, close to $\phi_c$, one infers from Fig. 2 that the stress-signal is highly intermittent showing a coexistence between the two states of yield-stress and zero-stress Newtonian flow. Note, the striking similarity with the stress-strain curves of the experiments of Behringer *et al.* (see e.g. [15]).

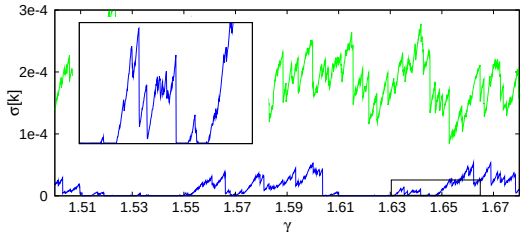


FIG. 2: Stress-strain relation for a sample of 2500 particles at two different volume fractions, $\phi = 0.8470, 0.8433$.

We have counted the number of jamming-events that lead from the zero-stress flow to the yield-stress flow at finite stress, and back (see Fig. 3). At high volume fractions the system always flows at finite stress so no event occurs. The same is true at low volume fractions where the system always flows at zero stress. Thus, we expect a maximum at an intermediate volume fraction $\phi_c$ where the system is highly unstable and makes frequent transitions between the two types of flows. For increasing system size we find the width of the coexistence region to decrease, presumably vanishing in the thermodynamic limit. The extrapolated peak position, $\phi_c(\infty) = 0.8433 \pm 0.0003$, can thus be used to define a critical density. At this volume-fraction the system develops a yield-stress and the flow changes from being "liquid-like" to "solid-like".

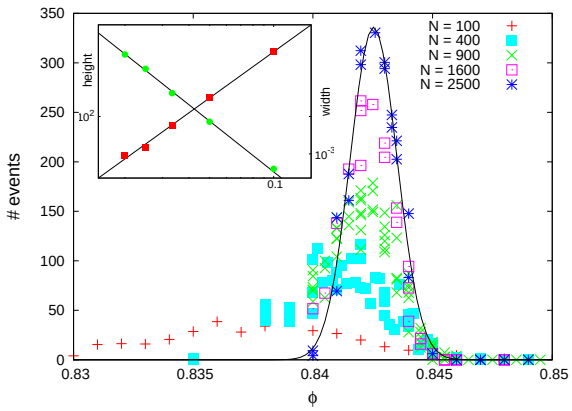


FIG. 3: Number of jamming events (defined as states where stress first exceeds a threshold value, $\sigma_{\rm thresh} = 2e-07$) as function of volume fraction $\phi$ and system size $N$. Inset: Finite-size scaling indicates a vanishing width and a diverging height as $N \to \infty$.

The results obtained here are similar to the finite-size scaling in Ref. [1]. There is an important difference, however. In that study statistical information is gathered by generating initial states that are as random as possible. The observable is the probability that such a randomly chosen state is jammed. In contrast, here we are concerned with states that are connected by the trajectory of the system itself. We are quantifying a dynamical transition rate at which the system, in the course of shear, undergoes a jamming transition.

One may view the equilibrated finite-stress states visited during the flow ($\phi > \phi_c$) as an ensemble of jammed states that is generated, not by an external protocol, but by the energy landscape itself. In this spirit we have analyzed the elastic branches and found good agreement with previously identified anomalous scaling properties characteristic of marginally rigid solids. In particular, we found the shear modulus $g$ to scale with the square root of pressure, $g \sim p^{1/2}$ (not shown). Note, however, that this shear modulus is *not* the linear elastic modulus of the system $g(\sigma = 0) \equiv g_{\rm lin}$, as discussed in Ref. [1]. Rather, it is defined at (or just below) the yield-stress, $g = g(\sigma = \sigma_y)$. As the yield-stress itself is pressure dependent (we find $\sigma_y \sim p$) the modulus may in fact show a complicated dependence on pressure, $p$. This is not the case, however, if we assume $g$ to take the scaling form, $g(\sigma, p) = p^{1/2} F(\sigma/\sigma_y(p))$. At the yield stress, the argument of the scaling function is a constant and we recover $g \sim p^{1/2}$ just as at zero stress. Note, that the presence of a scaling function $F$ is to be expected close to point J. It has furthermore explicitly been evidenced in the elastic network model of Ref. [16].

Another hallmark of marginally rigid solids is the scaling of the contact number, $z$. In agreement with the sce-

nario under decompression we find, $\delta z \equiv z - z_0 \sim p^{1/2}$ (see Fig. 4). The number of contacts at zero pressure, $z_0 \approx 3.8$, is slightly smaller than the isostatic value, as rattlers have not been accounted for [20]. The scaling has been shown to result from a competition between two terms in an expansion of the elastic energy, $W \sim k u_\parallel^2 - p u_\perp^2$ [17]. In this expression, $u_\parallel$ denotes the change in compression of a particle contact, while $u_\perp$ relates to the rotation of the two particles around each other. It has been shown ([6, 7]) that both displacement components are related by $u_\parallel \sim u_\perp \delta z$, such that the energy can be written as, $W/u_\perp^2 \sim k\delta z^2 - p$. Thus, both terms are of the same size, when $\delta z^2 \sim p$, which is the scaling relation observed numerically.

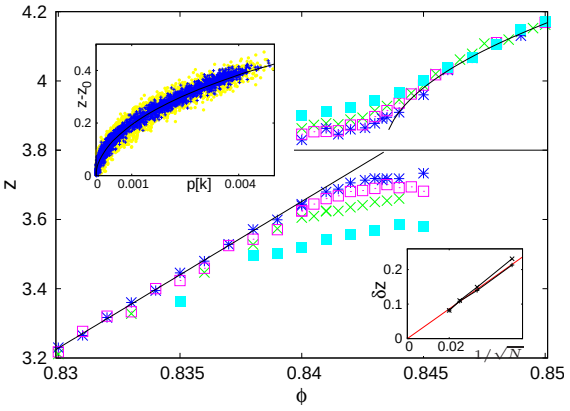


FIG. 4: Contact number $z$ as function of pressure (left inset) and volume-fraction $\phi$ (main panel). Symbols are as in Fig. 3. Right inset: scaling of gap width, $\delta z_{gap} \equiv 3.8 - z$, with system-size for $\phi = 0.844, 0.843$.

In decompression simulations, the number of contacts displays a discontinuity at $\phi_c$ and jumps from the isostatic value, $z_0$, to zero. This reflects the absence of any dynamics that would rearrange the particles once they have lost contact. In contrast, steady shear as studied with the quasistatic simulation leads to structural rearrangements and thus to particle contacts even at low volume fractions below $\phi_c$. As can be seen in Fig. 4, there is still a gap in the number of contacts between jammed finite-stress (upper branch) and zero-stress (lower branch) configurations. However, this is just a sampling artifact and reflects the tendency for jammed configurations to have $z > z_0$, while zero-stress states generally have $z < z_0$. As can be verified in the inset, the width of the gap is reduced with increasing the system size and seems to vanish in the thermodynamic limit, where only states at $z_0$ are sampled.

Furthermore, we find (see Fig. 4) that below $\phi_c$ the number of contacts simply increases *linearly* with volume-fraction, $\delta z \sim \delta\phi$, in striking contrast with the square-root behavior found above $\phi_c$. The resulting cusp at $\phi_c$ is illustrated in the figure. The different scaling above and below suggest that different mechanisms are responsible for the formation of contacts. Indeed, the energetic competition that controls the number of contacts in the jammed system is absent below $\phi_c$, where contact formation is of purely geometric origin (the excluded volume of the particles). Interestingly, this also implies that the isostatic length-scale $l^\star \sim |\delta z|^{-1}$ scales differently with volume-fraction above and below jamming. To define $l^\star$ below $\phi_c$, note, that an isostatic cluster can be equilibrated by blocking its "surface" degrees of freedom. The scale $l^\star$ is then defined (similarly as above $\phi_c$ [6, 7]) as the size of clusters, in which the number of extra degrees of freedom in the bulk (due to missing contacts, $\delta z l^{\star d}$) is comparable to the number of surface degrees of freedom, $l^{\star d-1}$.

To summarize this part, we find the ensemble of solid states at the yield-stress, $\sigma_y(\phi)$, to display the scaling laws characteristic of marginally rigid solids. As the contact number does not show a discontinuity at $\phi_c$ we should view jamming under shear as a conventional continuous transition, in contrast with the mixed character ascribed to the transition seen under decompression.

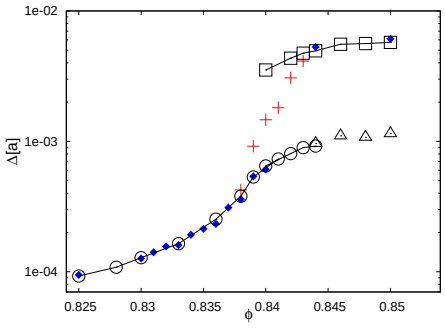


FIG. 5: Non-affine displacements $\Delta$ ($N = 900$) taken from: average over all configurations (red plus), restricted average over flowing states (circles), jammed states (square) and jammed states without plastic events (triangles). (Small closed symbols) flowing/jammed states at $N = 1600$.

This continuity is also present on the single-particle level as we will discuss now. For non-interacting particles, the particle displacements are affine, $\mathbf{u} = \gamma x \hat{\mathbf{e}}_\mathbf{y}$ (for shear in y-direction). Interactions lead to additional non-affine motion, in particular to a non-zero $x$-component, $u_{\rm na} \equiv \mathbf{u} \cdot \hat{\mathbf{e}}_\mathbf{x}$. In Fig. 5 we display $\Delta \equiv \langle u_{\rm na}^2 \rangle^{1/2}$ as a function of volume fraction, $\phi$.

We find perfect continuity of the particle displacements across $\phi_c$ *only* if we exclude the plastic events from the average and consider the displacements either in the reversible elastic states (triangles) or the states at zero-stress (circles). Plastic events are, in general, violent rearrangements that span the whole system. Consequently, these events dominate the amplitude of the mean-square displacement in the finite-stress states (squares).

From the continuity of the displacements we conclude

that the mechanism that leads to nonaffine motion in the ensemble of solid states above $\phi_c$ is the same as that in the fluid flow just below $\phi_c$. The difference being that above $\phi_c$ particle motion leads to the build-up of stress and its subsequent release in the plastic events. Apparently, this does not affect the magnitude of the (elastic) non-affine displacements. However, it *does* show up in their correlations.

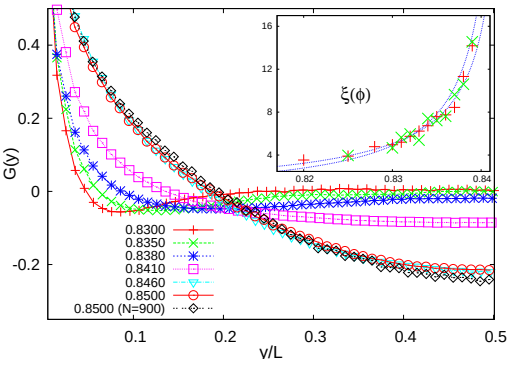


FIG. 6: Correlation function $G(y)$ ($N = 2500$) for various volume-fractions above and below $\phi_c$. For $\phi \lessapprox \phi_c$ correlations do not decay to zero, probably due to the peridiodicity of the simulation box. Inset: Length-scale $\xi$ as defined by the position of the minimum. Dashed lines are $\sim \delta\phi^{-0.8}$ and $\sim \delta\phi^{-1}$ ($\phi_c = 0.8433$).

Following Ref. [10] we study the correlation function $G(\mathbf{r}) = \langle u_{\rm na}(\mathbf{r}) u_{\rm na}(0)\rangle$ taken at $\mathbf{r} = \hat{\mathbf{e}}_{\mathbf{y}} y$, thus pointing along the shear direction. As in Ref. [10] we find a minimum of the correlation function in the freely flowing phase ($\phi < \phi_c$). The corresponding length-scale $\xi(\delta\phi)$ grows with approaching the critical volume fraction from below. Unfortunately, extracting a reliable value for the correlation length exponent $\nu$ is hampered by the restricted range of only one order of magnitude. Values may range from $\nu = 0.8 \ldots 1.0$ as indicated in the inset of Fig. 6 (no fit). Note, that a data fit would be highly sensitive to the value of $\phi_c$ used. This may also be the reason why previous studies report smaller values, $0.6 \ldots 0.7$ [10, 18]. With an exponent of $\nu = 1$ this may indeed be the isostatic length-scale, $\xi \equiv l^\star \sim \delta z^{-1} \sim \delta\phi^{-1}$, thus, indicating the presence of isostatic clusters that grow on approaching $\phi_c$ from below.

A quite different behavior is found in the regime above $\phi_c$. Here $G(y)$ does not have a minimum and always decays monotonously. The relevant length-scale is the system-size, $\xi \sim L$. This is consistent with findings in Ref. [19] where the lack of observable length-scale is explained with the dominance of long-range elastic couplings that place yield-stress flows automatically into a system-size dominated regime.

These results suggest the following picture for the flow at small strain-rates: the flow properties at small (and zero) stress and volume-fractions below $\phi_c$ are governed by the vicinity to the isostatic state. This is evidenced by a correlation length that diverges on approaching the isostatic point J from below. As a consequence, one may view the flow as due to the rearrangements of a liquid of marginally rigid, isostatic clusters. Close to point J a cross-over takes the system to a different regime ($\phi > \phi_c$), where the flow properties are dominated by long-range elastic interactions. This regime, thus, reflects the physics of amorphous, but well connected, materials, where flow is due to the irreversible rearrangements of liquid-like defects in a solid matrix.

The authors acknowledge fruitful discussions with Pinaki Chauduri and Ludovic Berthier, as well as thank the von-Humboldt Feodor-Lynen, the Marie-Curie Eurosim and the ANR Syscom program for financial support.

[1] C. S. O'Hern, L. E. Silbert, A. J. Liu, and S. R. Nagel, Phys. Rev. E **68**, 11306 (2003).
[2] H. A. Makse, N. Gland, D. L. Johnson, and L. M. Schwartz, Phys. Rev. Lett. **83**, 5070 (1999).
[3] T. S. Majmudar, M. Sperl, S. Luding, and R. P. Behringer, Phys. Rev. Lett. **98**, 058001 (2007).
[4] C. F. Moukarzel, Phys. Rev. Lett. **81**, 1634 (1998).
[5] A. V. Tkachenko and T. A. Witten, Phys. Rev. E **60**, 687 (1999).
[6] M. Wyart, S. R. Nagel, and T. A. Witten, Europhys. Lett. **72**, 486 (2005).
[7] M. Wyart, L. E. Silbert, S. R. Nagel, and T. A. Witten, Phys. Rev. E **72**, 51306 (2005).
[8] S. Henkes and B. Chakraborty, Phys. Rev. Lett. **95**, 198002 (2005).
[9] J. M. Schwarz, A. J. Liu, and L. Chayes, Europhys. Lett. **73**, 560 (2006).
[10] P. Olsson and S. Teitel, Phys. Rev. Lett. **99**, 178001 (2007).
[11] T. Hatano, J. Phys. Soc. Jpn. **77**, 123002 (2008).
[12] P.-E. Peyneau and J.-N. Roux, Phys. Rev. E **78**, 011307 (2008).
[13] T. K. Haxton and A. J. Liu, Phys. Rev. Lett. **99**, 195701 (2007).
[14] http://lammps.sandia.gov/index.html.
[15] R. P. Behringer, D. Bi, B. Chakraborty, S. Henkes, and R. R. Hartley, Phys. Rev. Lett. **101**, 268301 (2008).
[16] M. Wyart, H. Liang, A. Kabla, and L. Mahadevan, Phys. Rev. Lett. **101**, 215501 (2008).
[17] W. G. Ellenbroek, E. Somfai, M. van Hecke, and W. van Saarloos, Phys. Rev. Lett. **97**, 258001 (2006).
[18] J. A. Drocco, M. B. Hastings, C. J. Reichhardt, and C. Reichhardt, Phys. Rev. Lett. **95**, 088001 (2005).
[19] C. E. Maloney, Phys. Rev. Lett. **97**, 035503 (2006).
[20] We have also performed simulations with rattlers defined as particles with zero contacts. The resulting estimate for $z_0$ is much closer to the expected value of 4.